UIT Report Vol. 12, No.2, pp.271~287, 1981 연구논문집 제 12권 제 2호 pp.271~287. 1981

A Study on the Electron Momentum Densities in Copper and Copper Alloy*

Sang Kyun Nha
Dept. of Applied Physics
(Received April 10, 1981)

〈Abstract〉

The electron momentum densities of Cu and Cu_{90} Ni_{10} alloy have been studied through the calculation of the Compton profile of photon. The Hartree-Fock-Slater electronic wave functions were used to calculate the electron momentum wave functions, the radial density distributions, and then the Compton profiles. It was shown that the Compton profiles have some rather discontinuous changes in the slopes due to the contributions from momentum densities of the electronic shells. It was also shown that the top of the Compton profiles was mainly governed by the momentum densities of the outermost electrons. It was suggested here that the electron behaviour of the outermost electrons in matter, which is of most physical and chemical interest, can be studied, under proper experimental resolution, by measurement of the line shape of the top of peak of the Compton profile.

銅 및 銅合金 電子運動量 密度 硏究

羅 商 均
應 用 物 理 學 科
(1981. 4. 10 접수)

〈요 약〉

光子의 Compton profile을 計算하여 Cu 및 Cu_{90} Ni_{10} 合金의 電子運動量 密度를 硏究하였다. Hartree-Fock-Slater 電子波動函數를 利用하여 電子運動量函數와 동경密度分布를 計算하고 이들을 利用하여 Compton Profile을 計算하였다. 本 硏究는 Compton Profile이 各電子軌道의 電子運動量密度에 따라 그 기울기가 變하고 있음을 보여 주었다. 또한 Compton Profile의 웃部分은 電子軌道의 最外각 軌道電子의 運動量密度에 크게 依存되고 있음을 보여 주었다. 따라서 이 Compton Profile의 웃部分이 適當한 分解能의 實驗으로서 測定될 때 化學 및 物理的으로 가장 關心이 많은 物質內 最外각電子의 運動狀態가 硏究될 수 있음을 暗示하여 주고 있다.

I. Introduction

During the past few years studies of the electronic momentum distributions in atoms, molecules, and crystals have always been an interesting problem. The electronic momentum densities, which are useful for the study of Fermi surface, can be determined by a class of method employing three types of sentitive studies: The

* Supported by the Ministry of Education, Republic of Korea.

positrom annihilation studies, the quasi free scattering of electrons, and the Compton profile studies of photon [1)-3)].

In this work the method of the Compton profile studies was used for the study of the electronic momentum densities of copper and its alloy. The choice of copper as a material to be studied was made, for this work, by the requirement that a large amount of information concerning its electronic momentum densities, experimental as well as theoretical, is available from other sources [4)-6)] in order to allow a comparison of the results obtained.

In Compton scattering the scattered photon energy depends on the velocity of the electron providing the scattering because of the Doppler effect produced by the moving electron. Therefore a study of the Compton profiles provide a direct insight into the electron momentum distribution and thus the electronic momentum densities of the scattering materials. Since the momentum spectrum of the electrons is directly related to the electron wave functions, knowledge about the wave functions is also obtained by such investigations.

Recently, several new experimental methods [7)-9)] have been developed to study the Compton scattered photon spectra in matter and sufficient knowledge on the experimental shape of the Compton scattering is now accumulated, from which the information about the electron momentum distributions can be obtained. Very little theoretical work[10)], however, has been done on the momentum distributions of electrons in matter, despite their importance and intrinsic interest. The reason for scarcity of theoretical work lies in the nature of the calculations. Owing to the complicated form of the potential energy in the Hamiltonian of the system, it was known not to be practicable to use the p-representation to obtain the momentum distribution functions, but it was desired to use the Dirac transformation theory with space wave functions. This has brought the further complication that the knowledge of the precise space wave functions of electrons has always been scanty. Fortunately, very accurate electronic wave functions are now available from the Hartree-Fock-Slater work [11)], where the Computer methods were used to obtain self-consistant solution of the Hartree-Fock-Slater wave equations based on the free-electron exchange approximation. This therefore enables us to use the electronic wave functions for the calculations of the Compton profiles of copper and its alloy.

It is necessary to relate each calculated Compton profile to the measured one for the study of the electron momentum distributions which produced the spectrum. Since the experimental data now available are not sufficiently detailed to determine the electron momentum distribution directly with high precision, the inverse procedure will be used in this work: the electron momentum densities are first assumed and then the Compton profiles resulting from this distribution will be calculated.

Ⅱ. Theoretical Spectra

1. Electronic Wave Functions

Electronic wave functions of the Hartree-Fock-Slater theory were used for this work. The Hartree-Fock-Slater theory for the atomic structure calculation is Slater's simplified version of the Hartree Fock equations based on the free-electron exchange approximation.

The radial Hatree-Fock-Slater wave equations for a free atom can be written in the following form:

$$\left[-\frac{d^2}{dr^2}+\frac{m(m+1)}{r^2}+V(r)\right]rR_{lm}(r)=E_{lm}rR_{lm}(r) \qquad (1)$$

where l is the principal quantum number, m is the orbital quantum number, and $V(r)$ is the

sum of the nuclear Coulomb petential, the total electronic Coulomb potential, and the exchange potential such as

$$V(r)=V_0(r)=-\frac{2Z}{r}-\frac{2}{r}\int_0^r\sigma(t)dt$$
$$-2\int_0^\infty\frac{\sigma(t)}{t}dt-\sigma\left[-\frac{3}{8\pi}\rho(r)\right]^{\frac{1}{3}}, \quad (2)$$

where, Z is the atomic number, and $\rho(r)$ is the spherically averaged total electronic charge density and can be expressed as

$$\rho(r)=\frac{\sigma(r)}{4\pi r^2}, \text{ where } \sigma(r)=-\Sigma_{lm}w_{lm}[rR_{lm}(r)]^2 \quad (3)$$

with w_{lm} being the occupation number for the orbital lm. Since the principal computational difficulty posed by the Hartree-Fock equations is the treatment of the exchange terms, it was pointed out by Slater that the Hartree-Fock exchange potentials for different occupied orbitals, through different from one another in detail, in many respects and the essential feature of the Hartree-Fock method could be retained by replacing the exchange potentials for different orbitals by a universal exchange potential formed suitably averaging these individual exchange potentials.

The numerical values of the normalized radial wave function generated from the Hartree-Fock-Slater self-consistent theory were plotted as shown in Figs 1 and 2 for copper and nickel atoms. The $Cu_{90}Ni_{10}$ alloy wave functions is assumed to be described by the free atomic wave functions for Cu (90%) and Ni(10%). The electronic wave functions of $Cu_{90}Ni_{10}$ alloy were, thus, obtained by assuming that the Cu and Ni wavefunctions were superposed for the CuNi alloy wave functions. Fig. 3 shows the $Cu_{90}Ni_{10}$ alloy electronic wave functions.

Electronic configurations of copper and nickel are as follows:

shell	K	L		M			N	Total No. of Electrons
electron state	1s	2s	2p	3s	3p	3d	4s	
Cu	2	2	6	2	6	10	1	29
Ni	2	2	6	2	6	8	2	28
	2	2	6	2	6	9	1	28

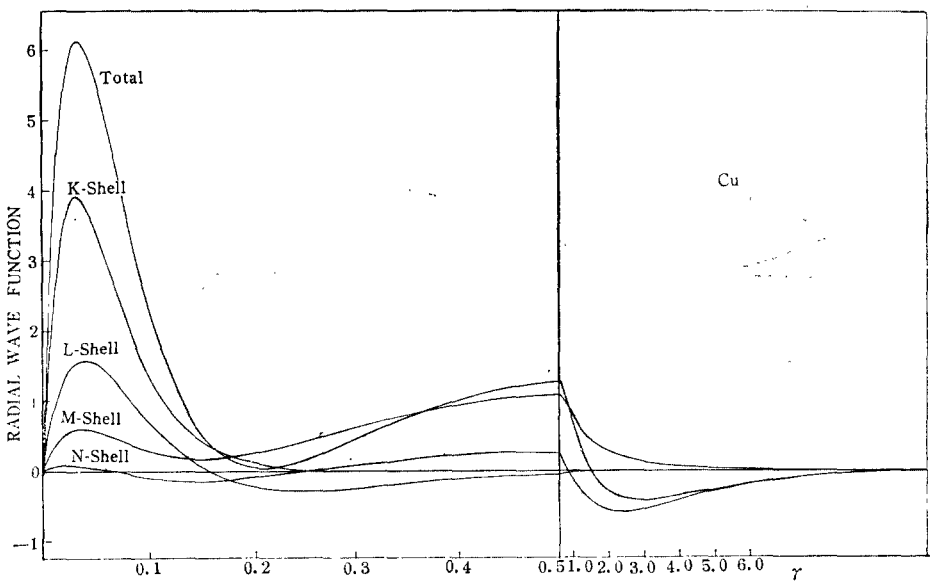

Fig. 1 Electronic wave function of Cu-atom calculated by the Hartree-Fock-Slater theory.

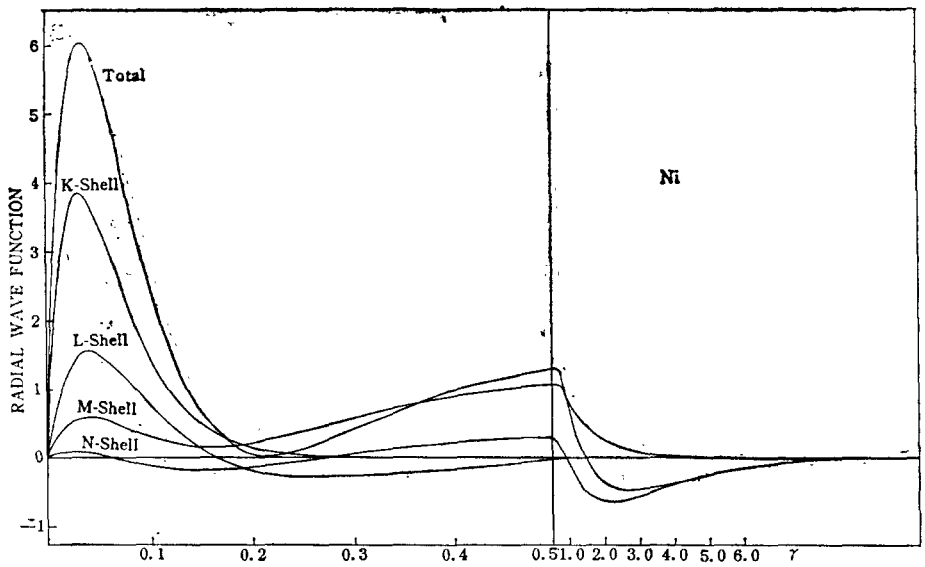

Fig. 2 Electronic wave function of Ni-atom calculated by the Hartree-Fock-Slater theory.

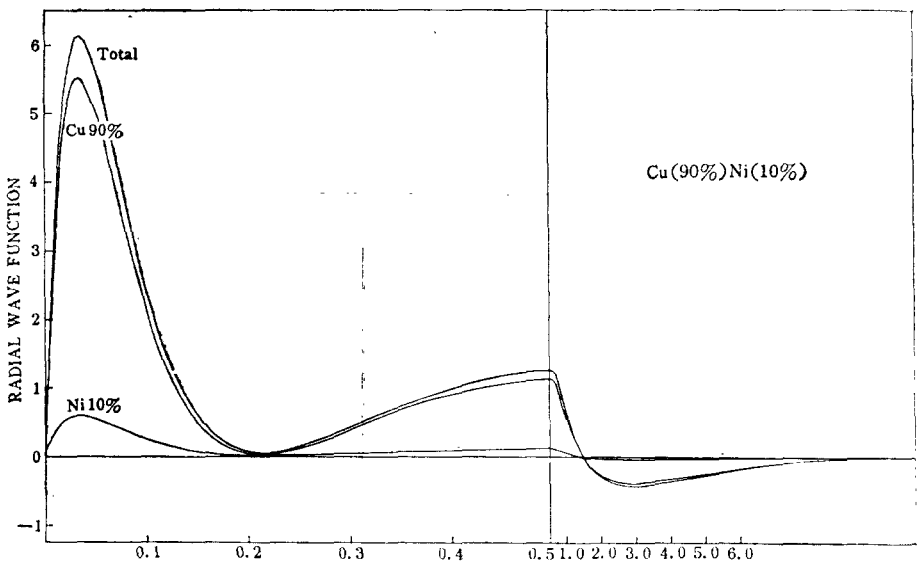

Fig. 3 Electronic wave function of $Cu_{90}Ni_{10}$ atom calculated by the Hartree-Fock-Slater theory. The $Cu_{90}Ni_{10}$ alloy electronic wave function is superposed by the electronic wave functions of Cu(90%) and of Ni(10%).

Here, the ground state configuration of nickel is listed by $3d^84s^2$ and $3d^94s^1$. Griffith[12] appeared to prefer $3d^94s^1$ because the average energy of the lowest multiplet of $3d^94s^1$ is less than the average energy of the lowest multiplet of $3d^84s^2$. Moore[13] appears to favor $3d^84s^2$ because the lowest term level is one arising from the lowest multiplet of $3d^84s^2$. The $3d^84s^2$ electronic

configuration of Ni was chosen for this work.

2. Electron Momentum Distributions.

If the electronic space wave function for a single orbital of (lmn) state is ϕ_{lmn}, then its electronic momentum wave function $F_{lmn}(\vec{p}\ (p,\Theta,\Phi))$ through the use of nonrelativistic transformation theory is given by

$$F_{lmn}(\vec{p}(p,\Theta,\Phi))=\frac{1}{(2\pi\hbar)^{3/2}}\times\int\exp\left(-\frac{i\vec{p}\cdot\vec{r}}{\hbar}\right)\phi_{lmn}(\vec{r})d\vec{r}, \quad (4)$$

where n is the azimuthal quantum number.

The electronic momentum density $\rho(\vec{p})$ is then given by the absolute square of the electronic momentum wave function, that is, the probablity of finding momentum lying between p_x, p_y, p_z and p_x+dp_x, p_y+dp_y, and p_z+dp_z:

$$\rho(\vec{p})=|F_{lmn}(\vec{p})|^2. \quad (5)$$

Usually the electronic momentum density of Eq. (5) is extended in the Hartree-Fock formalism to include the contributions from all occupied orbitals by writing

$$\rho(\vec{p})=\sum_{i=1}^{\text{occ.}}|F_{lmn,i}(\vec{p})|^2. \quad (6)$$

Since the scattering atoms are oriented in a random fashion, the quantity required is its probablity $\omega_{lm}(p)$ of the electron having a momentum lying between p and $p+dp$ when the atoms have been averaged over all angles Θ and Φ. This quantity is simply the average of $|F_{lmn}(\vec{p})|^2$ over all angles multiplied by p^2:

$$\omega_{lm}(p)=\frac{1}{2\pi}\int_{+1}^{+1}d(\cos\Theta)\times\int_0^{2\pi}d\Phi p^2|F_{lmn}(p,\Theta,\Phi)|^2. \quad (7)$$

For all the electrons occupied orbitals, then

$$\omega(p)=\sum_l\sum_m\omega_{lm}(p) \quad (8)$$

or in terms of β,

$$\omega(\beta)=m_0c\omega(p). \quad (9)$$

The calculation of $\omega(\beta)$ is carried out as follows: The wave functions $\phi_{lmn}(\vec{r})$ of the electrons are expanded in terms of spherical harmonics $Y^n{}_m(\theta,\phi)$

$$\phi_{lm}(\vec{r})=a_{lm}(\vec{r})Y^n{}_m(\theta,\phi) \quad (10)$$

the a_{lm} are the radial electronic wave functions tabulated in the previous section. Denoting the angle between $\vec{r}(r,\theta,\phi)$ and $\vec{p}(p,\Theta,\Phi)$ by α and introducing $\vec{k}=\frac{\vec{p}}{\hbar}$, an expansion is made of the exponential term in Eq. (4):

$$e^{-ikr\cos\alpha}=\sum_{j=0}^{\infty}(2j+1)(-i)^j\left(\frac{\pi}{2kr}\right)^{\frac{1}{2}}J_{j+\frac{1}{2}}(kr)\times p_j(\cos\alpha), \quad (11)$$

where $J_{j+\frac{1}{2}}$ is a Bessel function of the first kind of the order of $j+\frac{1}{2}$ and p_j a Legendre polynomial of order j. The addition theorem for $p_j(\cos\alpha)$ gives, also,

$$p_j(\cos\alpha)=\frac{\pi}{2j+1}\sum_{m'=-j}^{j}Y_j^{m'}(\Theta,\Phi)Y_j^{m'*}(\theta,\phi), \quad (12)$$

where $\alpha=\Theta-\theta$.

Substituting Eqs. (10), (11) and (12) into Eq. (4), the expression for the momentum wave function $F_{lmn}(\vec{p})$ becomes

$$F_{lmn}(\vec{p})=\frac{1}{(2\pi\hbar)^{\frac{3}{2}}}\int_0^{\infty}r^2dr\int_{-1}^{+1}d(\cos\theta)\int_0^{2\pi}d\phi a_{lm}(r)\times Y_m{}^n(\theta,\phi)\sum_{j=0}^{\infty}(2j+1)(-i)^j\left(\frac{\pi}{2kr}\right)^{\frac{1}{2}}\times J_{j+\frac{1}{2}}(kr)\frac{4\pi}{2j+1}\sum_{m'=-j}^{j}Y_j^{m'}(\Theta,\Phi)Y_j^{m'*}(\theta,\phi) \quad (13)$$

Integrating over the angles and using the ort hogonal properties of the $Y^n{}_m$ functions, the expression for $F_{lmn}(p,\Theta,\Phi)$ becomes

$$F_{lmn}(p,\Theta,\Phi)=\left(\frac{2}{\pi}\right)^{\frac{1}{2}}\int_0^{\infty}r^2dr(-i)^na_{lm}(r)j_m(kr)\times Y_m{}^n(\Theta,\Phi), \quad (14)$$

where the spherical Bessel function $j_j(\rho)=\left(\frac{\pi}{2\rho}\right)^{\frac{1}{2}}J_{j+\frac{1}{2}}$ has been introduced. Eq. (14) is then used to calculate $F_{lmn}(p,\Theta,\Phi)$ for the values of $a_{lm}(r)$ for the different electrons in copper atom and its alloy $Cu_{90}Ni_{10}$. The electron momentum distributions, $\omega(\beta)$, which follows directly from Eq. (14) and (7) to (9), then, were computed from the tabulated values of $a_{lm}(r)$ obtained from a Hatree-Fock-Slater theory.

Figs. 4, 5, and 6 show the electron momentum wave function calculated for Cu, Ni, and $Cu_{90}Ni_{10}$ alloy. The electron momentum distribution of $Cu_{90}Ni_{10}$ alloy was assumed to be superposed from the electron momentum distributions of $Cu_{(90\%)}$ and $Ni_{(10\%)}$ atoms.

The electronic momentum density $\rho(\vec{p})$ is, thus, just as fundamental to the quantum mechanical description of a system as the more familiar electron density distribution $\rho(\vec{r})$. Indeed just as $\rho(\vec{r})$ can be written as the square of a probability amplitude or space wave function $\phi(\vec{r})$ so also can $\rho(\vec{p})$ be written as $|F(\vec{p})|^2$ as shown in Eq. (5), where $F(\vec{p})$ is the electron momentum wave function satisfying the same Schrödinger equation. The two wave functions are simply Fourier transforms of each other and a complete knowledge of one implies a complete knowledge of the other. The radial density distributions in Cu, Ni, and Cu_{90} Ni_{10} alloy in coordinate space and in momentum space are shown in Figs. 7, 8, and 9, respectively.

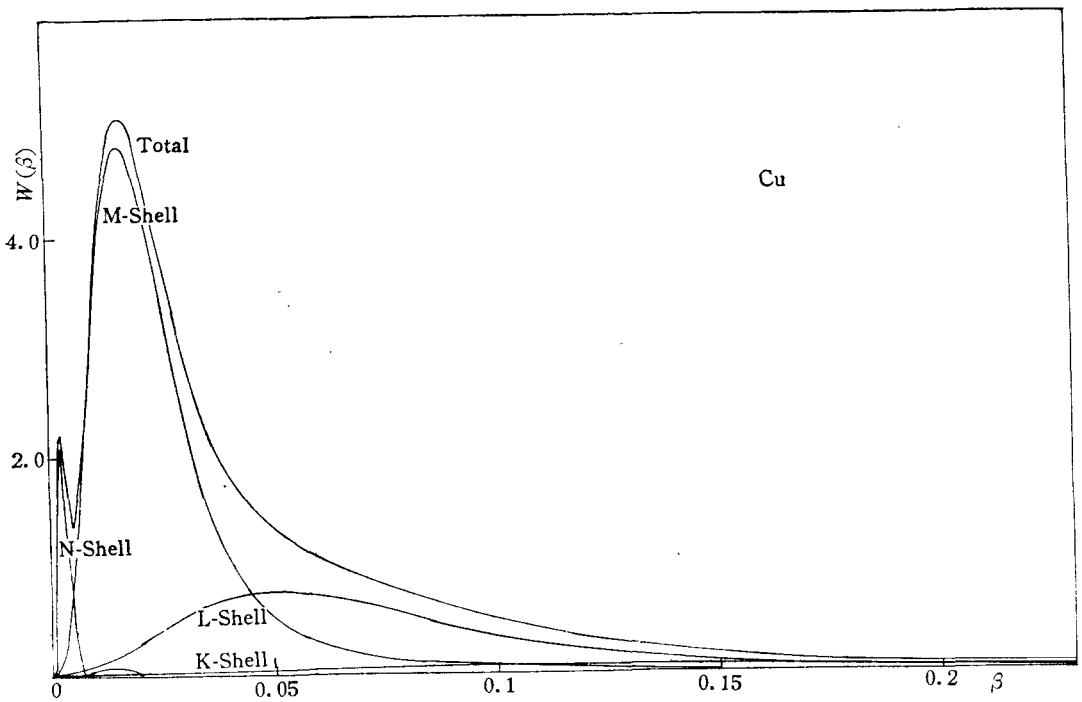

Fig. 4 Electronic Momentum Distribution in Cu-atom.

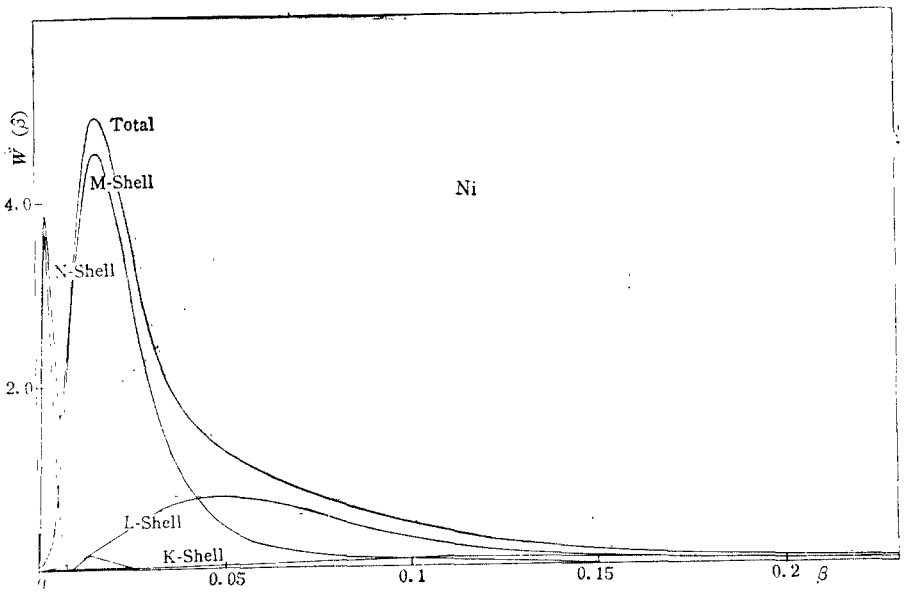

Fig. 5 Electronic Momentum Distribution in Ni-atom.

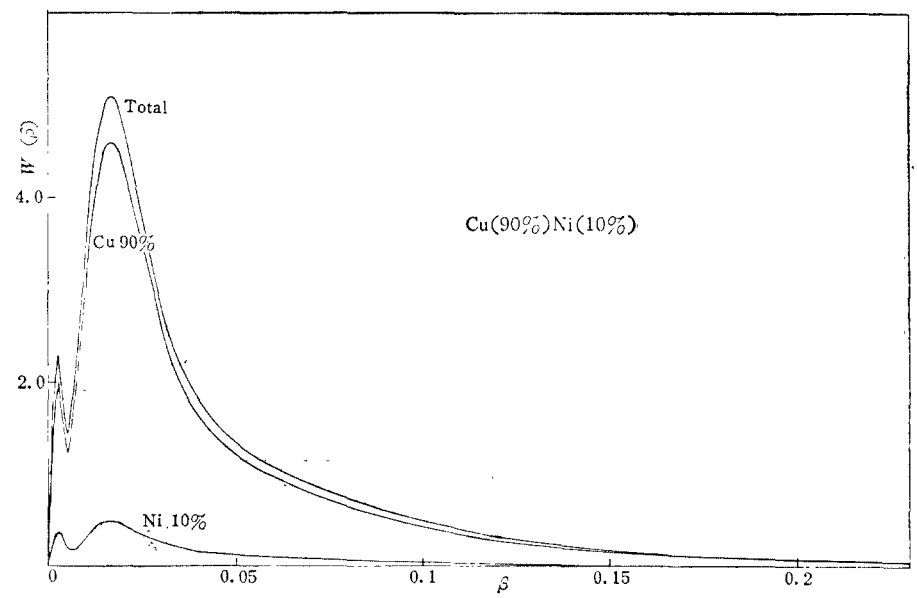

Fig. 6 Electronic Momentum Distribution in $Cu_{90}Ni_{10}$ alloy, which is superposed by the electronic momentum distributions of Cu(90%) and Ni(10%).

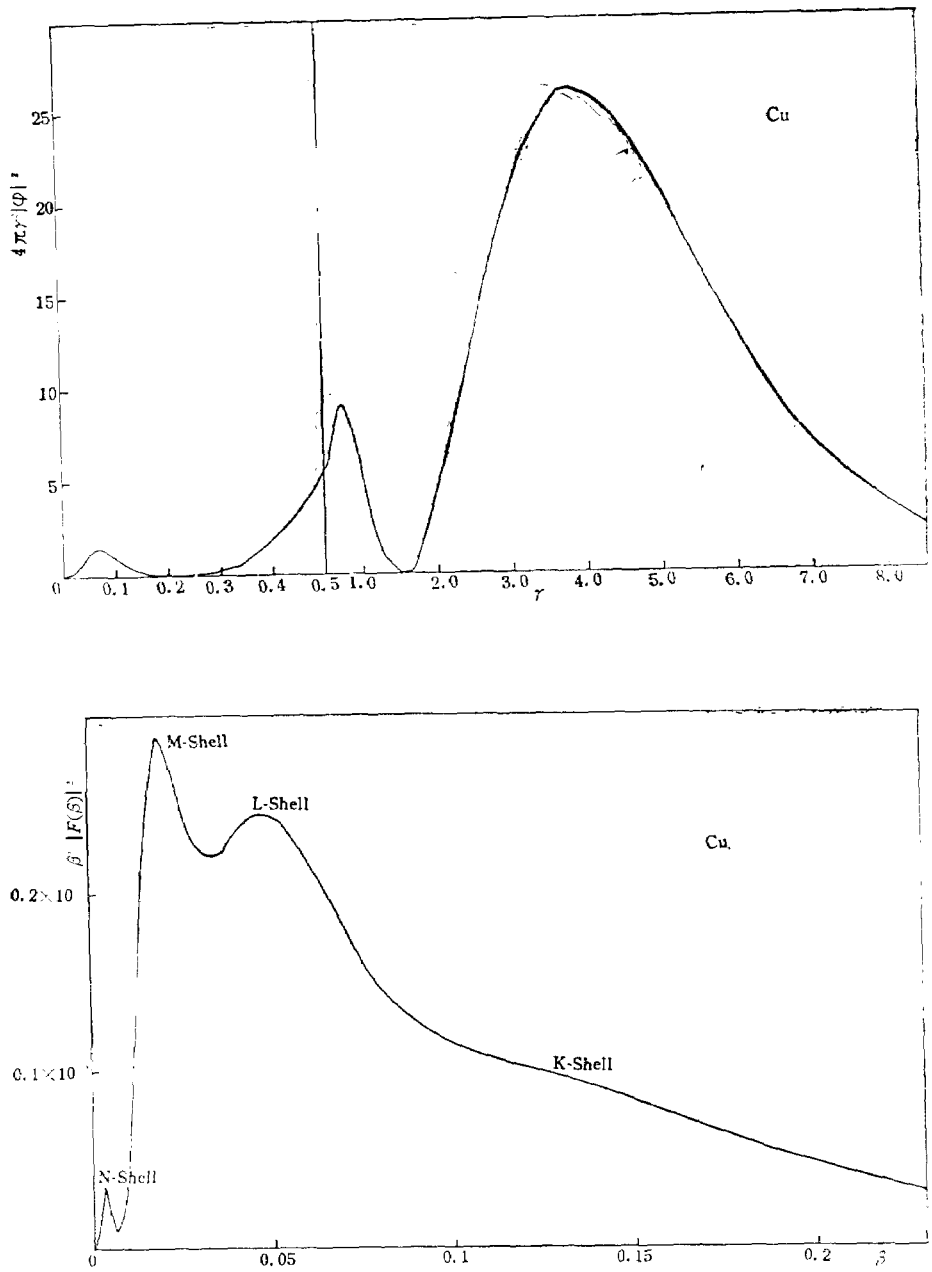

Fig. 7 The radial density distribution in Cu (a) in coordinate space and (b) in momentum space. The atomic unit (a.u.) of length is the Bohr radius, 0.53×10^{-10}m and the atomic unit of momentum is 2.7×10^{-24} Ns.

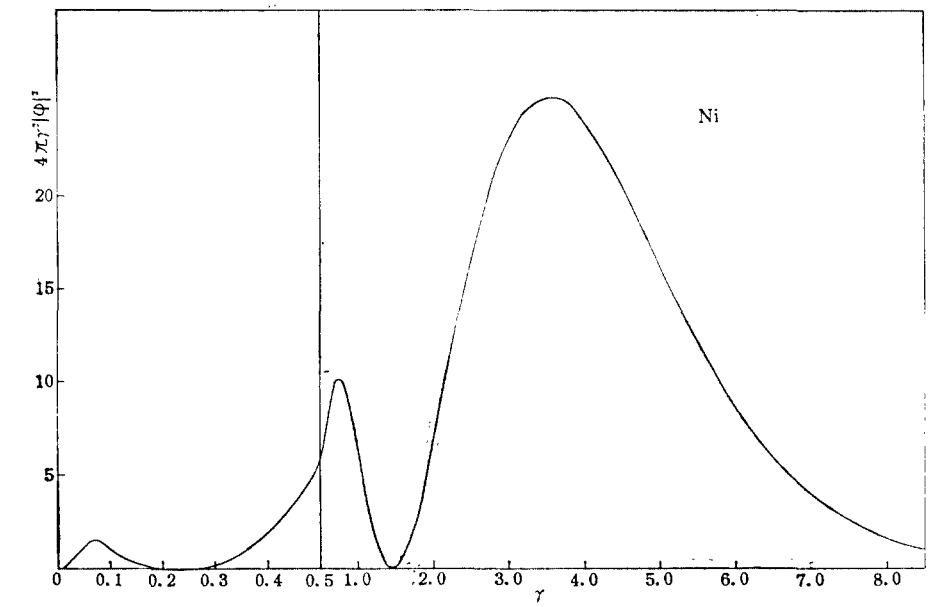

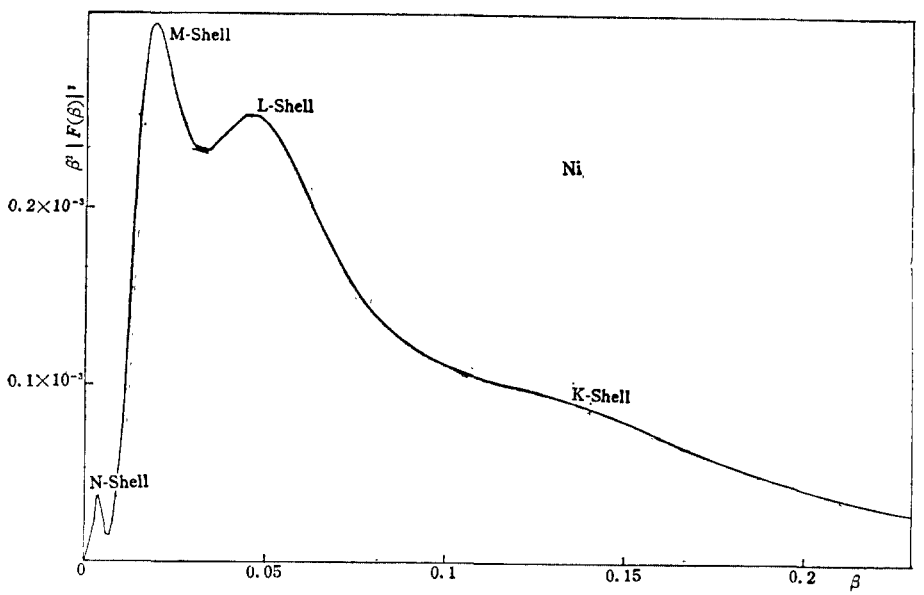

Fig. 8 The radial density distribution in Ni (a) in coordinate space and (b) in momentum space. The atomic unit (a.u.) of length is the Bohr radius, 0.53×10^{-10}m and the atomic unit of momentum is 2.7×10^{-24}Ns

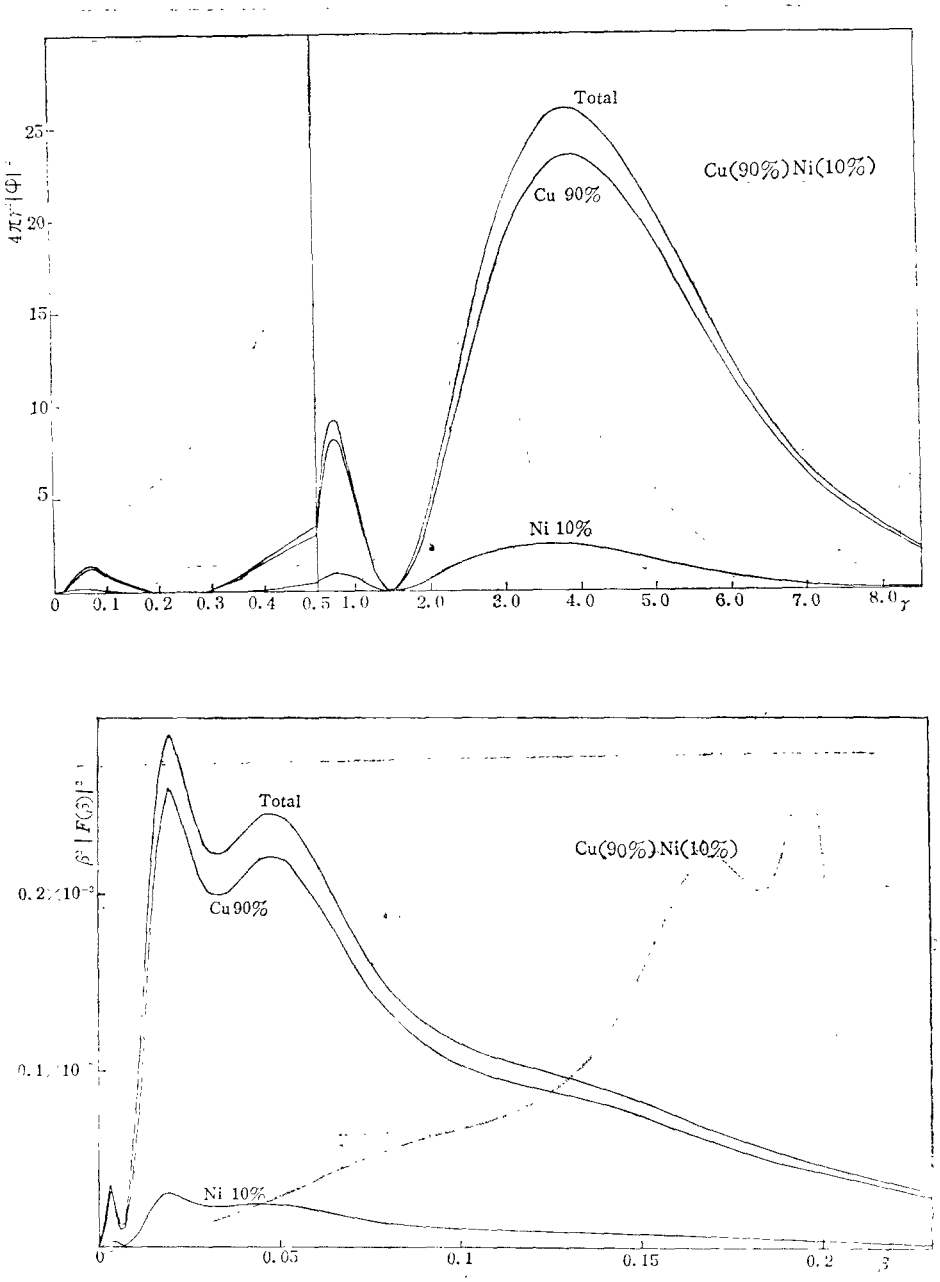

Fig. 9 The radial density distribution in $Cu_{90}Ni_{10}$ (a) in coordinate space and (b) in momentum space. The atomic unit (a.u.) of length is the Bohr radius, 0.53×10^{-10}m and the atomic unit of momentum is 2.7×10^{-24}Ns. The electron momentum distribution of $Cu_{90}Ni_{10}$ was superposed from the electron momentum distributions of Cu(90%) and Ni(10%).

3. Compton Profiles

Photons scattered from atomic electrons give rise to the Compton effect. It is usually described as the elastic collision of a photon with an electron. Thus a photon of wavelength λ_1, incident on a stationary, free electron is scattered to a wavelength λ_c at an angle θ. Laws of conservation of linear momentum and energy lead to the well-known formula for the Compton shift in the wavelength of the photon:

$$\lambda_c=\lambda_2(\beta=0)=\lambda_1+\frac{h}{m_0c}(1-\cos\theta), \qquad (15)$$

where $\frac{h}{m_0c}=0.02426$Å, the so-called Compton wavelength.

Two simplifying assumptions are made in deriving formula Eq. (15). These are: (i) the electron is free and (ii) the electron is at rest. The first assumption is valid as long as the kinetic energy of the recoiling electron is much larger than its binding energy in the atom. The second assumption is too simlified because we know that electrons in a solid have a continu ous distribution of momenta and thus they cannot be considered to be at rest. Eq. (15) is changed if one considers the electron to have an initial linear momentum. Because of the velocity of the electron there is shift in wavelength l of the scattered photon from its value λ_c: This shift can be expressed as

$$l=\lambda_2-\lambda_c=2\beta\lambda^*\frac{\cos\phi}{1-\beta\cos\theta_1}, \qquad (16)$$

where λ_2 is the scattered photon wavelength from the moving electron, θ_1 is the angle between the initial electron momentum and a new reference axis which lies in the direction of the change in momentum of the photon for the scattering from a stationary electron, while λ^* is defined by

$$2\lambda^*=(\lambda_c^2+\lambda_1^2-2\lambda_c\lambda_1\cos\theta)^{\frac{1}{2}}. \qquad (17)$$

The relation between θ_1 and ϕ is given by

$$\cos\theta_1=\sin\phi\cos\chi\sin\gamma+\cos\phi\cos\gamma, \qquad (18)$$

where χ is the azimuthal angle of the initial electron momentum measured from the scattering plan and

$$\cos\gamma=\frac{4\lambda^{*2}+\lambda_c^2-\lambda_1^2}{4\lambda_2\lambda^*} \qquad (19)$$

Thus for an incident photon of wavelength λ_1, Compton-scattered at certain angle θ from electrons in atom, the shift l in the wavelength is not given by a unique value but shows a Compton profile, which is a Doppler-broadened lineshape in the wavelength spectrum of the Compton-scattered radiation determined by Eq. (16).

The expression for l as a function of the variables of the problem is given by Eq. (15) through Eq. (19) and can be summarized by the expression:

$$l=\frac{2\beta\lambda^*(\lambda_1,\theta)\cos\phi}{1-\beta\cos\theta_1(\lambda_1,\theta,\cos\phi,\chi)}. \qquad (20)$$

The calculation of a Compton profile, $p(l)$, is as follows: To begin calculation of $p(l)$, λ_1 and θ are fixed. The value of $\beta=\left(\frac{v}{c}\right)$ is also kept fixed. Then only $\cos\phi$ and χ can vary and because of the isotropic distribution of electron velocities, $\bar{v}$, equal intervals in these vari ables are equally probable. In the calculation, then, a mesh of l-values was computed for equal intervals of χ and $\cos\phi$. By counting the number of boxes in the mesh where l-values were between l and $l+dl$, a quantity proportional to $p(l)$ was found.

The probability $p(l)$ was then calculated in a similar manner for many values of β so that $p(l,\beta)$ quantities were known. Each $p(l,\beta)$ was then weighted by $\omega(\beta)$, the probability that the electron velocity $\beta=\frac{v}{c}$ lies between β and $\beta+d\beta$ can be calculated. Thus, the final distribution in l was obtained:

$$p(l)dl=\int_0^\infty d\beta\omega(\beta)p(l,\beta)dl. \qquad (21)$$

The calculation was simplified by the empirical fact that $p(l,\beta)$ was found to be essentially constant for all values of l between $l_{min}(\beta)$ and $l_{max}(\beta)$ for a given β. Here, l_{min} and l_{max} are

the extreme values of l calculated from Eq. (20) for a given β. Thus,

$$\int_{l_{min}}^{l_{max}} p(l,\beta)dl \simeq p(l,\beta)(l_{max}-l_{min})=1 \qquad (22)$$

or

$$p(l,\beta)=\begin{cases}\dfrac{1}{l_{max}(\beta)-l_{min}(\beta)} & \text{for } l_{min}<l<l_{max}\\ 0, \text{otherwise.}\end{cases}$$

Substituting into Eq. (21)

$$p(l)=\int_{\beta_{min}}^{1}\frac{\omega(\beta)}{l_{max}(\beta)-l_{min}(\beta)}d\beta. \qquad (24)$$

Here, β_{min} is the smallest value such that a $p(l,\beta)\neq 0$. The $l_{max}(\beta)$and $l_{max}(\beta)$ are evaluated froms Eqs. (15) and (16) for $\cos\phi=\pm 1$:

$$l_{max}(\beta)=\frac{2\beta\lambda^*}{1-\beta\cos\gamma}$$

$$l_{min}(\beta)=\frac{-2\beta\lambda^*}{1+\beta\cos\gamma} \qquad (25)$$

and the values for β_{min} was expressed as follows:

$$\beta_{min}=\frac{l}{2\lambda^*+l\cos\gamma} \quad \text{for } l>0$$

$$\beta_{min}=\frac{-l}{2\lambda^*+l\cos\gamma} \quad \text{for } l<0 \qquad (26)$$

From Eq. (15) $l_{max}-l_{min}$ can also be evaluated and substituted into Eq. (23) to obtain

$$p(l)=\int_{\beta_{min}}^{1}d\beta\omega(\beta)\left[\frac{1-\beta^2\cos^2\gamma}{4\beta\lambda^*}\right] \qquad (27)$$

which permits the calculation of the wavelength spectrum of the Compton profile of the scattered photons.

In experiments, the energy spectrum of the Compton profile rather than the wavelength spectrum is usually measured and thus the wavelength spectrum, $p(l)$, should be converted into the energy spectrum of the Compton profiles, $p(\epsilon)$, such that

$$p(\epsilon)=-\frac{\lambda_c}{E_c}p(l) \quad \text{at a given angle } \theta, \qquad (28)$$

where ϵ is the energy displacement from the Compton scattering energy $E_c(\beta=0)$.

With the recent production of high specific activity Co_{60} material, it is now possible to

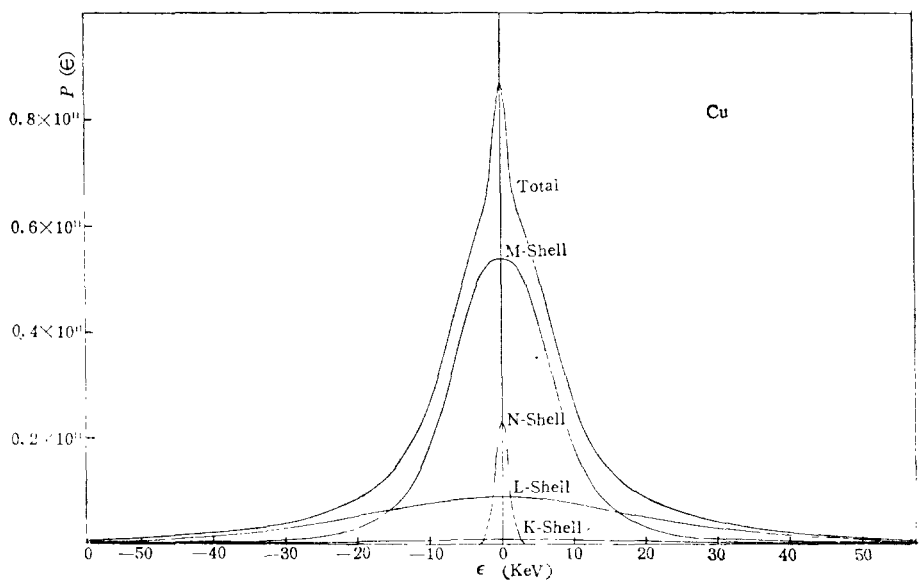

Fig. 10 Theoretical Compton profile of Cu-atom for photon energy 1.33 Mev at a scattering angle 30°.

perform the Compton scattering experiment at a photon energy of 1.33 Mev. The Compton profiles here calculated for copper and $Cu_{90}Ni_{10}$ alloy with a photon energy 1.33 Mev at a scattering angle 30°.

The calculated Compton profile for Cu are plotted in Fig. 10. Here, the total spectrum is shown along with the spectra for the contributions from the various electronic shells. Fig. 11 shows the Compton profile calculated for $Cu_{90}Ni_{10}$ alloy. It is just a superposition of the Compton profiles of Cu(90%) and Ni(10%) because the momentum distribution of $Cu_{90}Ni_{10}$ was assumed to be a superposition of the momentum distributions of Cu(90%) and Ni(10%).

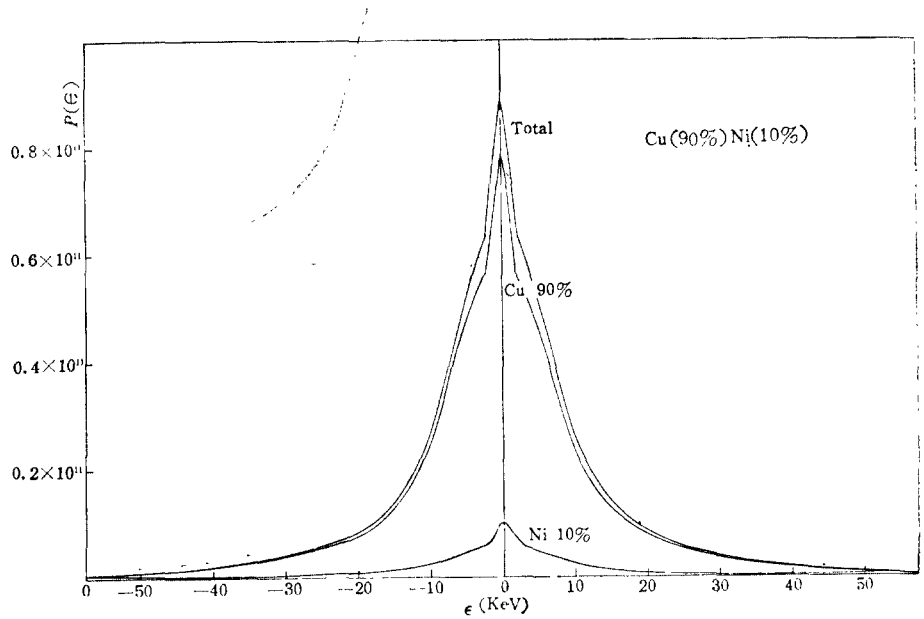

Fig. 11 Theoretical Compton profile of $Cu_{90}Ni_{10}$ alloy for the photon energy 1.33 Mev at a scattering angle 30°. The Compton profile of $Cu_{90}Ni_{10}$ alloy was considered to be a superposition of the Compton profiles of Cu(90%) and Ni(10%).

4. Scattering by Free Electrons

For metals, the electrons in the outer electronic shells are considered to be not bound to the atom but move throughout the metal. If these electrons are assumed to be free and two electrons are permitted in each energy state (due to the two possible orientations of the electronic spin and the Pauli exclusion principle), then by counting the number of filled boxes of dimension h^3 lying with momentum up to p_F, the Fermi momentum, it is clear that

$$\frac{n}{2}h^3=\frac{4\pi}{3}p_F^3V, \tag{29}$$

where n is the number of free electrons and V is the volume of the material. Thus, the Fermi momentum, p_F, can be expressed as

$$p_F=\frac{h}{2}\left(\frac{3}{\pi}\rho\right)^{\frac{1}{3}}, \tag{30}$$

where ρ is the number of free electrons per unit volume. The probability $w(p)dp$ of an electron having a momentum between p and $p+dp$ is then volume of a spherical shell of radius p and thickness dp:

$$w(p)dp=\begin{cases}\left(\frac{3}{p_F^3}\right)p^2dp & \text{for } 0<p<p_F\\ 0 & \text{for } p>p_F\end{cases} \tag{31}$$

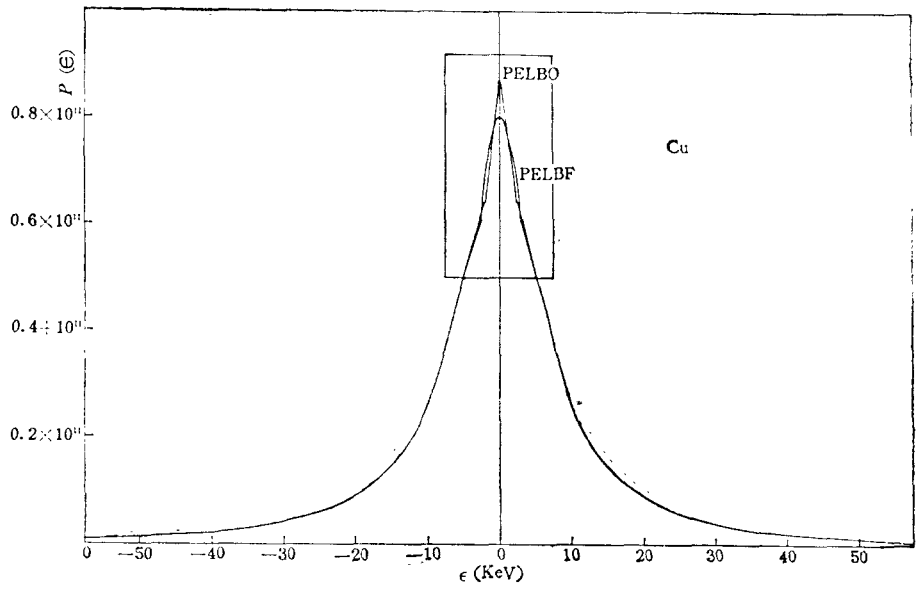

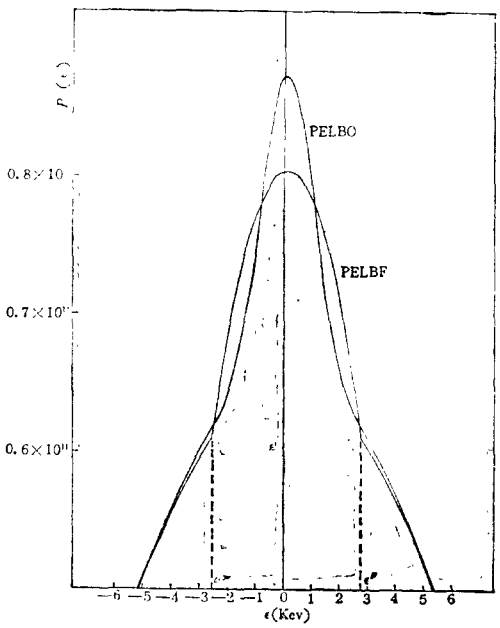

Fig. 12 The theoretical Compton profile of Cu atom calculated by assuming that one outer shell electron as a free elec tron and as a bound electron, which were superposed on the Compton profile of the bound electrons in Cu. The Compton profiles are so normalized that the area under the peak has the same area. p_F is the Fermi momentum.

or

$$w(\beta)=\begin{cases} m_0 c w(p) & \text{for } \beta<\beta_F \\ 0 & \text{for } \beta>\beta_F. \end{cases} \qquad (32)$$

The theoretical Compton profile for the free electrons in a scattering material can now be generated by using Eq. (32) and Eq. (31) along with Eq. (27).

Fig. 12 shows the Compton profile of Cu atom in metal calculated for one free electron in Cu whose the electron momentum distributi on was calculated by Eq. (32) together with Compton profile of one outer shell electron momentum distribution calculated from Eq. (14) using the Hartree-Fock-Slater electronic wave functions. Here, the Compton profile of one free electron calculated in free electron theory has been normalized to contain the same area under the peak with that of the electron in the outer electronic shell.

Ⅲ. Discussion of Results.

1. Electron Behaviour in Momentum Space

In general it can be said that it is possible and proper to describe electron beha viour in

atoms, molecules and solids in terms of $F(\vec{p})$ and $\rho(\vec{p})$. Indeed it is necessary to do so in order to underestand how useful information can be extracted from Compton profiles which are directly related to the electron momentum densities. In free atoms the principle - the building up of atoms by adding successive electrons into energy levels with due regard for the Pauli exclusion principleis the accepted starting point for the constru ction of the periodic table of elements, based on the hydrogenic model, i.e. using the quantum numbers l, m, and n obtained in the hydrogen atom solution. The result is a picture of shells of electrons starting with the innermost, the K shell, and moving radially outwards through the L and M shells and so on. This model is clearly indicated if one sees the radial density distribution $4\pi r^2\rho(r)$ which is shown for Cu in Fig.7 (a): the shells are clearly located. Now if, alternatively, the radial density distribution in momentum space, $4\pi p^2\rho(p)$, is plotted against p, the shell structure is still visible, but the outer of the shells is reversed (see Fig 7 (b)). The K shell, which was sharply defined in coordinate space is now diffuse whereas the N shell shows the reverse tendency, the sharpest features belong to the outermost electrons, which are of course those of most physical and chemical interest. The nickel atom and Cu_{90} N_{10} alloy have also the same electron behaviour as copper's as shown in Figs 8 and 9.

However, in crystalline solids at least the idea of a momentum representation is not such a novelty as it appeared for atoms. They are invariably described in terms of the band structure in k-space, where $\hbar k$ is referred to as the "crystal momentum". Indeed in the free electron model of metals the eigenstates are momentum eigenstates and $\vec{p}$ and $\vec{k}$ are equivalent ($\vec{p}=\hbar\vec{k}$). At absolute zero the free electron Fermi distribution is sphere of radius $p_F(=\sqrt{2mE_F})$ centered at the origin in momentum space with all states below the surface full and all those above empty. Since there are of the order 10^{23} states uniformly distributed in k-space, the momentum distribution is well-described by a sphere radius p_F, of uniform density.

The Compton profile of the free electron in Cu is as shown in Fig.12, an inverted parabola of the form. The most obvious aspect of this distribution, namely, the cut-off at $\epsilon=\pm\epsilon_F$, which is $p=p_F$, appeared as shown in Fig.12, and thus the Compton profile in practice provides a method of measuring of the Fermi diameter, $2p_F$.

2. Shapes of Compton Profiles

1) Inner electron shells

It is seen from the Compton profiles of Figs. 10 and 11 for Cu and $Cu_{90}Ni_{10}$ alloy that different shells tend to contribute different parts of the total spectrum. There are some rather discontinuous changes in the slopes of the sides of the totalspectrum due to the contributions from other shells. The principal features of the Compton line shape (e.g. the full width at half maximum) are effectively governed by the behaviour of the outer electrons: the core electrons merely provide a relatively slowly-varing background contribution. Because of the high velocity and small number of these electrons, their contribution to the scattered photon energy spectrum is diffuse and small, and also it could be possible to interfere with the experimental background. Thus the "core" portion of the Compton profiles becomes larger and tightly bound electrons provide a broad and flat contribution to the profile. However, the study of the contribution of these inner electrons would be extremely difficult particularly because the effects of these electrons are shifted because of their binding energy to the low energy side of the peak.

Furthermore, for a heavier atom with more electrons and more tightly bound, the shells move in towards the origin in coordinate space, but out from the origin in momentem space in acc ordance with the Heisenberg uncertainty principle which is, of course, embodied in the Fourier transform relationship between the wave functions in the two spaces.

If there is appearance of such features in an experimental spectrum, they can be used to give information about the electron velocity distributions in the various electronic shells.

2) Outer electron shells and free electrons.

The spectra in Figs. 10 and 11 are particularly sensitive to the velocities in the outer elecctron shells. These velocities are low and hence give the least broadening to the spectrum peak. They contribute, therefore, to the top of the peak which can be the most easily measured feature of the peak. However, as shown in Fig. 10 and 11, the widths of the spectrum contributed by the outer shell electrons is only about 2.4 keV for Cu and 2.6 keV for $Cu_{90}Ni_{10}$ alloy, respectively. Thus, if one wants to measure to study the structure of these peaks, and instrumental resolution considerably better than these values is required. For the case of the instru mental resolution larger than these values such structure could not be measured. The instrumental resolution in fact will even wash out the break in the spectrum.

The free electron in Cu, as shown in Fig. 12, has clearly a distinct difference with the line shape for the outer electron. The difference of the line shapes in width is approximately 0.5 keV, so that, again this difference is not considered to be demonstrated experimentally because the present instrumental resolution is known to be poor to allow the measurement of these effects.

Ⅳ. Conclusions

It has been shown for Cu and $Cu_{90}Ni_{10}$ alloy that the Compton profile has some rather discontinuous change in the slopes due to the contributions from the momentum densities of each electronic shell electrons. The Compton profile of the outermost electrons, whose feature of the radial density distribution is the sharpest in momentum space and is diffuse in positive space, has been shown to be very sensitive and the least broadening, while Compton profile of the tightly bound electrons has been found to be relatively bread and flat. It has also shown that the difference in the line shape of the top of the peak of the Compton profileoue to two different theories on "free electron" and "outer electron" about the outermost shell electron is very distinct.

Thus, the principal features of the Compton profile are directly related and effectively governed by the electron momentum densities of the electronic shell electrons. It was suggested that, under experimental resolution less than kev, the top of the Compton profile can be measured and thus the information about the electron momentum densities and the electron behaviour can also be obtained.

Thus, the Compton profile studies can be said to be most useful for the study of the electron momentum densities of the inner shell electrons as well as the outermost electronic shell electrons.

〈Acknowledgments〉

I wish to thank Mr. Jong H. Kim for arranging my use of the computer at the Hyundai Heavy Industries, Co., LTD. I am also grateful to Mr. Cheol Mo Son, for his assistance in computer calculations.

References

1. R. Currat, P. D. DeCicco, and Roy Kaplow, Phys. Rev. B **3**, 243(1971)
2. Yasunori Kubo, Shinya Wakoh and Jiro Yamashita, J. Phys. Soc. Japan **41**, 830 (1976).
3. R. M. Singru, Phys. Stat. Sol. (a) **30**, 11 (1975)
4. P. E. Mijnarends, Phys. Rev. **178**, 622(1969).
5. Takashi. Akahane and Kunio Fujiwara, J. Phys. Soc. Japan **35**, 1660 (1973).
6. John D. McGervey, Phys. Rev. **9** 2402(1974)
7. S. K. Nha and J. A. McIntyre, Am J. Phys **40**, 1618 (1972)
8. Malcolm J. Cooper, Contemp Phys. **18**, 489 (1977).
9. J. P. Urban and R. Hosemmann, J. Appl. Phys, **49**, 392(1978).
10. Sinya Wakoh and Jiro Yamashita, J. Phys. Soc. Japan **35**, 1402(1973), Sinya Wakoh, Yasnnori Kubo, and Jiro Yamashita, J. Phys. Soc. Japan, **40**, 1043(1976).
11. F. Herman and S. Skillman, "Atomic Structure Calculations", Prentice-Hall, Englewood Cliffs, N. J. (1963).
12. J. S. Griffith, "The Theory of Transition Metal Ions", Cambridge University Press, Cambridge (1961).
13. C. E Moore, "Atomic Energy Levels" (Nati onal Bureau, of Standards Circular Number 467), Vol. 3(1958).